



Dynamic State Estimation for Radial Microgrid Protection

Arthur K. Barnes¹  *Member, IEEE* and Adam Mate¹  *Member, IEEE*

Abstract—Microgrids are localized electrical grids with control capability that are able to disconnect from the traditional grid to operate autonomously. They strengthen grid resilience, help mitigate grid disturbances, and support a flexible grid by enabling the integration of distributed energy resources. Given the likely presence of critical loads, the proper protection of microgrids is of vital importance; however, this is complicated in the case of inverter-interfaced microgrids where low fault currents preclude the use of conventional time-overcurrent protection. This paper introduces and investigates the application of dynamic state estimation, a generalization of differential protection, for the protection of radial portions of microgrids (or distribution networks); both phasor-based and dynamic approaches are investigated for protection. It is demonstrated through experiments on three case-study systems that dynamic state estimation is capable of correctly identifying model parameters for both normal and faulted operation.

Index Terms—power system operation, dynamic state estimation, microgrid, distribution network, protection.

I. INTRODUCTION

Dynamic state estimation (abbr. DSE) is a generalization of differential protection, which offers a reduced likelihood of misoperation, particularly in the case of assets with nonlinear characteristics (e.g., transformers that are being energized) [1]. It is also useful in cases where distance protection performs poorly (e.g., transmission lines with series compensation [2] or mutually coupled transmission lines [3]). DSE has previously been introduced to microgrid branch protection [4]–[6].

This paper investigates the application of DSE for the protection of radial portions of a microgrid (or a distribution network). This can be a challenge in electrical grids with distributed generation on account of lack of fault current from inverter-interfaced generation [7], varying fault current between grid-connected and islanded modes [7], and the potential for normally-meshed operation [8] and unbalanced operation due to single-phase loads [8]. Admittance relaying has been investigated as a solution for the protection of microgrids [9], however, it has been observed to present issues with grounded-wye connected loads [10]; consequently, additional relaying is necessary to prevent misoperation [8].

This paper treats the radial portions of a microgrid as load busses. It is assumed that these portions contain no loops or downstream generation; they are modeled as constant-impedance networks with unknown impedances but known connectivity. To ensure that the number of measured variables

is greater than approximately 1.6 times the number of free parameters (where 1.6 is a commonly selected number for redundancy to ensure sufficient measurements for system identification [11], [12]), most models presented here make the assumption that the loads are balanced.

Every load and fault configuration requires a separate model. For a given load configuration, a model for each fault configuration is fit to measured values; the model with the lowest error, in terms of fitting the observed variables, is assumed to be the correct one. On a grounded-wye-connected load, the following models are necessary to distinguish between normal operation, line-ground faults and line-line faults:

- 1) Normal operation: each branch of the load has the same impedance, which is modeled as a series resistive-inductive (abbr. RL) network.
- 2) Phase A-ground fault: the faulted branch A is modeled as a resistance, while the unfaulted branches B and C are modeled as series RL networks with equal parameters.
- 3) Phase B-ground fault: the faulted branch B is modeled as a resistance, while the unfaulted branches C and A are modeled as series RL networks with equal parameters.
- 4) Phase C-ground fault: the faulted branch C is modeled as a resistance, while the unfaulted branches A and B are modeled as series RL networks with equal parameters.
- 5) Phase A-B fault: the fault impedance is modeled as a resistance across the load terminals A and B, while each branch of the load is modeled as a series RL network.
- 6) Phase B-C fault: the fault impedance is modeled as a resistance across the load terminals B and C, while each branch of the load is modeled as a series RL network.
- 7) Phase C-A fault: the fault impedance is modeled as a resistance across the load terminals C and A, while each branch of the load is modeled as a series RL network.

On a delta-connected system, the following models are necessary to distinguish between normal operation, line-ground and line-line faults:

- 1) Normal operation: each branch of the load has the same impedance, which is modeled as series RL network.
- 2) Phase A-ground fault: the fault impedance is modeled as a resistance between load terminal A and ground, while the load branches are modeled as series RL networks.
- 3) Phase B-ground fault: the fault impedance is modeled as a resistance between load terminal B and ground, while the load branches are modeled as series RL networks.
- 4) Phase C-ground fault: the fault impedance is modeled as a resistance between load terminal C and ground, while the load branches are modeled as series RL networks.
- 5) Phase A-B fault: the fault impedance is modeled as a resistance across the load terminals A and B, while the branches across load terminals B-C and C-A are modeled as series RL networks.

Manuscript submitted: December 14, 2020.

¹ The authors are with the Advanced Network Science Initiative at Los Alamos National Laboratory, Los Alamos, NM 87544 USA. Email: {abarnes, amate}@lanl.gov.

Color versions of one or more of the figures in this paper are available online at <https://ieeexplore.ieee.org>.

LANL ANSI LA-UR-20-30126.

- 6) Phase B-C fault: the fault impedance is modeled as a resistance across the load terminals B and C, while the branches across load terminals C-A and A-B are modeled as series RL networks.
- 7) Phase C-A fault: the fault impedance is modeled as a resistance across the load terminals C and A, while the branches across load terminals A-B and B-C are modeled as series RL networks.

Both phasor-based and dynamic approaches are investigated for radial microgrid protection. Section II describes the implementation of phasor-based state estimation: it is conceptually similar to DSE but more straightforward to derive and implement as it only requires a single time period. Section III describes the implementation of DSE. Section IV describes how two different transient models of loads are developed as test cases and run to test both phasor and dynamic state estimation; next, Section V presents the performance of state estimation on the test cases. Finally, Section VI summarizes the conclusions of this paper.

II. PHASOR IMPLEMENTATION

The phasor implementation of state estimation-based protection is simpler: only a single time period is used, which limits the number of measurements and therefore the number of parameters that can be estimated. In this section, it is applied to single-phase, grounded-wye and delta-connected load configurations.

A. Single-Phase Impedance

The output of the system (illustrated in Fig. 1a):

$$\mathbf{y} = \begin{bmatrix} V \\ I \end{bmatrix}$$

where V and I are phasor quantities.

The state of the system:

$$\mathbf{x} = \begin{bmatrix} Z \\ I_z \end{bmatrix}$$

The output-state mapping for the system is the following vector-valued function:

$$\mathbf{y} = \mathbf{h}(\mathbf{x})$$

where

$$h_1(\mathbf{x}) = V_z = ZI_z \quad h_2(\mathbf{x}) = I_z$$

The Jacobian of $\mathbf{h}(\mathbf{x})$ is determined as follows:

$$\begin{aligned} \frac{\partial V_z}{\partial Z} &= \frac{\partial}{\partial Z} ZI_z = I_z & \frac{\partial V_z}{\partial I_z} &= \frac{\partial}{\partial I_z} ZI_z = Z \\ \frac{\partial I_z}{\partial Z} &= \frac{\partial}{\partial Z} I_z = 0 & \frac{\partial I_z}{\partial I_z} &= \frac{\partial}{\partial I_z} I_z = 1 \end{aligned}$$

The mapping between variables and the state vector:

$$Z = x_1 \quad I_z = x_2$$

Given the variable and state mapping, the Jacobian can be built as follows: $H(n, m) = 0$, unless specified below.

$$H = \begin{bmatrix} [1.5] \frac{\partial V_z}{\partial Z} & \frac{\partial V_z}{\partial I_z} \\ \frac{\partial I_z}{\partial Z} & \frac{\partial I_z}{\partial I_z} \end{bmatrix}$$

Given the Jacobian, the state of the system can be solved for iteratively:

$$\begin{aligned} \boldsymbol{\epsilon}_i &= \mathbf{y} - \mathbf{h}(\mathbf{x}_i) & J_i &= \|\boldsymbol{\epsilon}_i\|^2 \\ \mathbf{x}_{i+1} &= \mathbf{x}_i + (H_i' H_i)^{-1} H_i' \boldsymbol{\epsilon}_i \end{aligned}$$

B. Grounded-Wye with Line-Ground Fault

The output of the system (illustrated in Fig. 1b):

$$\mathbf{y} = [I_a \quad I_b \quad I_c \quad V_a \quad V_b \quad V_c]^T$$

The easiest way to model this is as an unbalanced load where the fault impedance is not treated specially. The state of the system therefore:

$$\mathbf{x} = [Y_a \quad Y_b \quad Y_c \quad V_{za} \quad V_{zb} \quad V_{zc}]^T$$

The output function $\mathbf{h}(\mathbf{x})$ can be written as:

$$\begin{aligned} \mathbf{h}_1(\mathbf{x}) &= I_a = y_a V_a & \mathbf{h}_2(\mathbf{x}) &= I_b = y_b V_b \\ \mathbf{h}_3(\mathbf{x}) &= I_c = y_c V_c & \mathbf{h}_4(\mathbf{x}) &= V_a = V_{za} \\ \mathbf{h}_5(\mathbf{x}) &= V_b = V_{zb} & \mathbf{h}_6(\mathbf{x}) &= V_c = V_{zc} \end{aligned}$$

C. Grounded-Wye with Line-Line Fault

The output of the system (illustrated in Fig. 1c):

$$\mathbf{y} = [I_a \quad I_b \quad I_c \quad V_a \quad V_b \quad V_c]^T$$

The state of the system:

$$\mathbf{x} = [Y_l \quad Y_f \quad V_{za} \quad V_{zb} \quad V_{zc}]^T$$

The output function $\mathbf{h}(\mathbf{x})$ can be written as:

$$\begin{aligned} h_1(\mathbf{x}) &= I_a = (y_l + y_f)V_{za} - y_f V_{zb} \\ h_2(\mathbf{x}) &= I_b = -y_f V_{za} + y_l V_{zb} \\ h_3(\mathbf{x}) &= I_c = y_l V_{zc} \\ h_4(\mathbf{x}) &= V_a = V_{za} \\ h_5(\mathbf{x}) &= V_b = V_{zb} \\ h_6(\mathbf{x}) &= V_c = V_{zc} \end{aligned}$$

D. Delta-Connected Load with Line-Line Fault

The output of the system (illustrated in Fig. 1d):

$$\mathbf{y} = [I_a \quad I_b \quad I_c \quad V_a \quad V_b \quad V_c]^T$$

The state of the system:

$$\mathbf{x} = [Y_f \quad Y_{ll} \quad V_{za} \quad V_{zb} \quad V_{zc}]^T$$

The output function $\mathbf{h}(\mathbf{x})$ can be written as:

$$\begin{aligned}
h_1(\mathbf{x}) &= I_a = y_{aa}V_{za} - y_{ab}V_{zb} - y_{ca}V_{zc} \\
&= (y_{ab} + y_{ca})V_{za} - y_{ab}V_{zb} - y_{ca}V_{zc} \\
&= (y_f + y_{ll})V_{za} - y_fV_{sb} - y_{ll}V_{zc} \\
h_2(\mathbf{x}) &= I_b = -y_{ab}V_{za} + y_{bb}V_{zb} - y_{bc}V_{zc} \\
&= -y_{ab}V_{za} + (y_{ab} + y_{bc})V_{zb} - y_{bc}V_{zc} \\
&= -y_fV_{za} + (y_f + y_{ll})V_{zb} - y_{ll}V_{zc} \\
h_3(\mathbf{x}) &= I_c = -y_{ca}V_{za} - y_{bc}V_{zb} + y_{cc}V_{zc} \\
&= -y_{ca}V_{za} - y_{bc}V_{zb} + (y_{ac} + y_{bc})V_{zc} \\
&= -y_{ll}V_{za} - y_{ll}V_{zb} + 2y_{ll}V_{zc} \\
h_4(\mathbf{x}) &= V_a = V_{za} \\
h_5(\mathbf{x}) &= V_b = V_{zb} \\
h_6(\mathbf{x}) &= V_c = V_{zc}
\end{aligned}$$

E. Delta-Connected Load with a Line-Ground Fault

The output of the system (illustrated in Fig. 1e):

$$\mathbf{y} = [I_a \quad I_b \quad I_c \quad V_a \quad V_b \quad V_c]^T$$

The state of the system:

$$\mathbf{x} = [Y_{ll} \quad Y_f \quad V_{za} \quad V_{zb} \quad V_{zc}]^T$$

The output function $\mathbf{h}(\mathbf{x})$ can be written as:

$$\begin{aligned}
h_1(\mathbf{x}) &= I_a = y_{aa}V_{za} - y_{ab}V_{zb} - y_{ca}V_{zc} \\
&= (y_{ab} + y_{ca} + y_{ag})V_{za} - y_{ab}V_{zb} - y_{ca}V_{zc} \\
&= (y_f + 2y_{ll})V_{za} - y_{ll}V_{sb} - y_{ll}V_{zc} \\
h_2(\mathbf{x}) &= I_b = -y_{ab}V_{za} + y_{bb}V_{zb} - y_{bc}V_{zc} \\
&= -y_{ab}V_{za} + (y_{ab} + y_{bc})V_{zb} - y_{bc}V_{zc} \\
&= -y_{ll}V_{za} + 2y_{ll}V_{zb} - y_{ll}V_{zc} \\
h_3(\mathbf{x}) &= I_c = -y_{ca}V_{za} - y_{bc}V_{zb} + y_{cc}V_{zc} \\
&= -y_{ca}V_{za} - y_{bc}V_{zb} + (y_{ac} + y_{bc})V_{zc} \\
&= -y_{ll}V_{za} - y_{ll}V_{zb} + 2y_{ll}V_{zc} \\
h_4(\mathbf{x}) &= V_a = V_{za} \\
h_5(\mathbf{x}) &= V_b = V_{zb} \\
h_6(\mathbf{x}) &= V_c = V_{zc}
\end{aligned}$$

III. DYNAMIC IMPLEMENTATION

While the phasor implementation uses a single time period for state estimation, with the dynamic implementation several periods are used; in this paper, 12 cycles are sampled at a 2 [kHz] sample rate. As in Section II, here the DSE-based protection is applied to single-phase, grounded-wye and delta-connected load configurations.

A. Single-Phase Series RL Load

The output of the system (illustrated in Fig. 2a):

$$y(t) = \begin{bmatrix} v(t) \\ i(t)z(t) \end{bmatrix}$$

For the purposes of state estimation, this is sampled at points $n \in \{1, \dots, N\}$ giving the following vector-value equation:

$$\mathbf{y} = \begin{bmatrix} \mathbf{v} \\ \mathbf{i} \end{bmatrix}$$

where

$$\begin{aligned}
\mathbf{v} &= [v(1) \quad v(2) \quad \dots \quad v(N)]^T \\
\mathbf{i} &= [i(1) \quad i(2) \quad \dots \quad i(N)]^T \\
\mathbf{z} &= [z(1) \quad z(2) \quad \dots \quad z(N)]^T
\end{aligned}$$

The state of the system:

$$\mathbf{x} = [R \quad L \quad \mathbf{v}_r \quad \mathbf{v}_l]^T$$

The output-state mapping for the system is the following vector-valued function:

$$\mathbf{y} = \mathbf{h}(\mathbf{x})$$

where

$$\begin{aligned}
h_n(\mathbf{x}) &= v_r(n) + v_l(n) \quad \forall n \in \{1, 2, \dots, N\} \\
h_{N+n}(\mathbf{x}) &= Gv_r(n) \quad \forall n \in \{1, 2, \dots, N\} \\
h_{2N+n}(\mathbf{x}) &= Gv_r(n) - Gv_r(n-2) + \frac{2\Lambda\Delta t}{6}(v_l(n) + \\
&\quad + 4v_l(n-1) + v_l(n-2)), \quad \forall n \in \{3, 4, \dots, N\}
\end{aligned}$$

In the above, $v_R(n) = Ri_L(n)$ follows from discretizing $v_R(t) = Ri_L(t)$, and

$$v_l(n) = \frac{2\Lambda\Delta t}{6}(v_l(n) + 4v_l(n-1) + v_l(n-2))$$

follows from discretizing

$$i_l(t) = \frac{1}{L} \int_{t-\Delta t}^t v_l(\tau) d\tau$$

via Simpson's 1/3 rule [13].

Given the variable and state vector mapping, the Jacobian can be built as follows: $H(n, m) = 0$, unless specified otherwise below.

$$\begin{aligned}
H(n, 2+n) &= \frac{\partial v(n)}{\partial v_r(n)} = 1 \quad \forall n \in \{1, 2, \dots, N\} \\
H(n, 2+N+n) &= \frac{\partial v(n)}{\partial v_l(n)} = 1 \quad \forall n \in \{1, 2, \dots, N\} \\
H(N+n, 1) &= \frac{\partial i(n)}{\partial G} = v_r(n) \quad \forall n \in \{1, 2, \dots, N\} \\
H(N+n, 2+n) &= \frac{\partial i(n)}{\partial v_r(n)} = G \quad \forall n \in \{1, 2, \dots, N\} \\
H(2N+n-2, 1) &= \frac{\partial z(n-2)}{\partial R} = v_r(n) - v_r(n-2) \\
&\quad \forall n \in \{3, 4, \dots, N\}
\end{aligned}$$

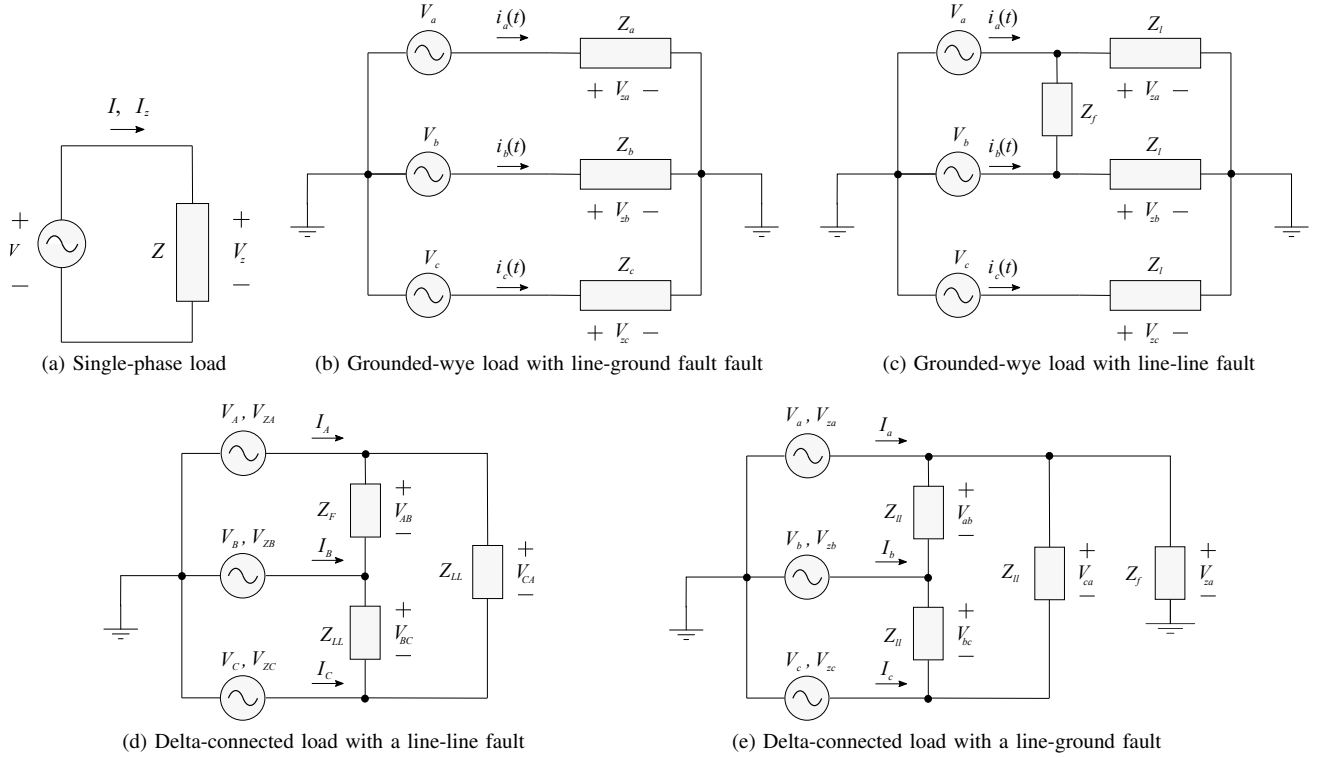


Fig. 1. Phasor-based implementation of state estimation-based protection, applied to single-phase, grounded-wye and delta-connected load configurations.

$$H(2N + n - 2, n) = \frac{\partial z(n-2)}{\partial v_r(n)} = G \quad \forall n \in \{3, 4, \dots, N\}$$

$$H(2N + n - 2, 2) = \frac{\partial z(n-2)}{\partial \Lambda} = \frac{2\Delta t}{6}(v_l(n) + 4v_l(n-1) + v_l(n-2)) \quad \forall n \in \{3, 4, \dots, N\}$$

$$H(2N + n - 2, 2 + N + n) = \frac{\partial z(n-2)}{\partial v_l(n)} = \frac{\Delta t \Lambda}{3} \quad \forall n \in \{1, 2, \dots, N\}$$

$$H(2N + n - 2, 1 + N + n) = \frac{\partial z(n-2)}{\partial v_l(n-1)} = \frac{4\Delta t \Lambda}{3} \quad \forall n \in \{1, 2, \dots, N\}$$

$$H(2N + n - 2, N + n) = \frac{\partial z(n-2)}{\partial v_l(n-2)} = \frac{\Delta t \Lambda}{3} \quad \forall n \in \{1, 2, \dots, N\}$$

Given the Jacobian, the state of the system can be solved for iteratively, by applying the same equations as in Section II-A.

B. Grounded-Wye Load without Fault

The sampled output of the system (illustrated in Fig. 2b):

$$\mathbf{y} = [\mathbf{v}_a \quad \mathbf{v}_b \quad \mathbf{v}_c \quad \mathbf{i}_a \quad \mathbf{i}_b \quad \mathbf{i}_c \quad \mathbf{z}_a \quad \mathbf{z}_b \quad \mathbf{z}_c]^T$$

where

$$\mathbf{v}_\phi = [v_\phi(1) \quad v_\phi(2) \quad \dots \quad v_\phi(N)]^T$$

$$\mathbf{i}_\phi = [i_\phi(1) \quad i_\phi(2) \quad \dots \quad i_\phi(N)]^T$$

$$\mathbf{z}_\phi = [z_\phi(1) \quad z_\phi(2) \quad \dots \quad z_\phi(N-2)]^T \text{ for } \phi \in \{a, b, c\}$$

The state of the system:

$$\mathbf{x}(t) = [G \quad \Lambda \quad \mathbf{v}_{ra} \quad \mathbf{v}_{rb} \quad \mathbf{v}_{rc} \quad \mathbf{v}_{la} \quad \mathbf{v}_{lb} \quad \mathbf{v}_{lc}]^T$$

where $G = R^{-1}$ is the conductance, $\Lambda = L^{-1}$ is the reciprocal of the inductance, $\mathbf{v}_{r\phi}$ is the voltage across the resistance on phase ϕ at each time period $1, \dots, N$ and $\mathbf{v}_{l\phi}$ is the voltage across the inductance on phase ϕ at each time period $1, \dots, N$.

The output function $\mathbf{h}(\mathbf{x})$ can be written as:

$$h_n(\mathbf{x}) = v_{ra}(n) + v_{la}(n) \quad \forall n \in \{1, 2, \dots, N\}$$

$$h_{n+N}(\mathbf{x}) = v_{rb}(n) + v_{lb}(n) \quad \forall n \in \{1, 2, \dots, N\}$$

$$h_{n+2N}(\mathbf{x}) = v_{rc}(n) + v_{lc}(n) \quad \forall n \in \{1, 2, \dots, N\}$$

$$h_{n+3N}(\mathbf{x}) = Gv_{ra}(n) \quad \forall n \in \{1, 2, \dots, N\}$$

$$h_{n+4N}(\mathbf{x}) = Gv_{rb}(n) \quad \forall n \in \{1, 2, \dots, N\}$$

$$h_{n+5N}(\mathbf{x}) = Gv_{rc}(n) \quad \forall n \in \{1, 2, \dots, N\}$$

$$h_{n+6N}(\mathbf{x}) = G(v_{ra}(n) - v_{ra}(n-2)) - \frac{2\Delta t \Lambda}{6}(v_{la}(n) + 4v_{la}(n-1) + v_{la}(n-2)) \quad \forall n \in \{1, 2, \dots, N\}$$

$$h_{n+7N}(\mathbf{x}) = G(v_{rb}(n) - v_{rb}(n-2)) - \frac{2\Delta t \Lambda}{6}(v_{lb}(n) + 4v_{lb}(n-1) + v_{lb}(n-2)) \quad \forall n \in \{1, 2, \dots, N\}$$

$$h_{n+8N}(\mathbf{x}) = G(v_{rc}(n) - v_{rc}(n-2)) - \frac{2\Delta t \Lambda}{6}(v_{lc}(n) + 4v_{lc}(n-1) + v_{lc}(n-2)) \quad \forall n \in \{1, 2, \dots, N\}.$$

C. Grounded-Wye Load with Line-Ground Fault

The sampled output of the system (illustrated in Fig. 2c):

$$\mathbf{y} = [\mathbf{v}_a \ \mathbf{v}_b \ \mathbf{v}_c \ \mathbf{i}_a \ \mathbf{i}_b \ \mathbf{i}_c \ \mathbf{z}_b \ \mathbf{z}_c]^T$$

Note that there are no $z_a(n)$ output variables as the reactive impedance on phase A is large compared to the parallel fault conductance G_f .

The state of the system:

$$x(t) = [G \ \Lambda \ G_f \ \mathbf{v}_{ra} \ \mathbf{v}_{rb} \ \mathbf{v}_{rc} \ \mathbf{v}_{lb} \ \mathbf{v}_{lc}]^T$$

where $G_f = R^{-1}$ is the conductance and the remaining states are the same as those in that of the grounded-wye no-fault state.

The output function $\mathbf{h}(\mathbf{x})$ can be written as:

$$\begin{aligned} h_n(\mathbf{x}) &= v_{ra}(n) \quad \forall n \in \{1, 2, \dots, N\} \\ h_{n+N}(\mathbf{x}) &= v_{rb}(n) + v_{lb}(n) \quad \forall n \in \{1, 2, \dots, N\} \\ h_{n+2N}(\mathbf{x}) &= v_{rb}(n) + v_{lb}(n) \quad \forall n \in \{1, 2, \dots, N\} \\ h_{n+3N}(\mathbf{x}) &= Gv_{ra}(n) \quad \forall n \in \{1, 2, \dots, N\} \\ h_{n+4N}(\mathbf{x}) &= Gv_{rb}(n) \quad \forall n \in \{1, 2, \dots, N\} \\ h_{n+5N}(\mathbf{x}) &= Gv_{rc}(n) \quad \forall n \in \{1, 2, \dots, N\} \\ h_{n+6N}(\mathbf{x}) &= G(v_{rb}(n) - v_{rb}(n-2)) - \frac{2\Delta t\Lambda}{6}(v_{lb}(n) + \\ &+ 4v_{lc}(n-1) + v_{lb}(n-2)) \quad \forall n \in \{1, 2, \dots, N\} \\ h_{n+7N}(\mathbf{x}) &= G(v_{rc}(n) - v_{rc}(n-2)) - \frac{2\Delta t\Lambda}{6}(v_{lc}(n) + \\ &+ 4v_{lc}(n-1) + v_{lc}(n-2)) \quad \forall n \in \{1, 2, \dots, N\} \end{aligned}$$

D. Grounded-Wye Load with Line-Line Fault

The sampled output of the system (illustrated in Fig. 2d):

$$\mathbf{y} = [\mathbf{v}_a \ \mathbf{v}_b \ \mathbf{v}_c \ \mathbf{i}_a \ \mathbf{i}_b \ \mathbf{i}_c \ \mathbf{z}_a \ \mathbf{z}_b \ \mathbf{z}_c]^T$$

The state of the system:

$$x(t) = [G \ \Lambda \ \mathbf{v}_{ra} \ \mathbf{v}_{rb} \ \mathbf{v}_{rc} \ \mathbf{v}_{la} \ \mathbf{v}_{lb} \ \mathbf{v}_{lc}]^T$$

The output function $\mathbf{h}(\mathbf{x})$ can be written as:

$$\begin{aligned} h_n(\mathbf{x}) &= v_{ra}(n) + v_{la}(n) \quad \forall n \in \{1, 2, \dots, N\} \\ h_{n+N}(\mathbf{x}) &= v_{rb}(n) + v_{lb}(n) \quad \forall n \in \{1, 2, \dots, N\} \\ h_{n+2N}(\mathbf{x}) &= v_{rb}(n) + v_{lb}(n) \quad \forall n \in \{1, 2, \dots, N\} \\ h_{n+3N}(\mathbf{x}) &= Gv_{ra}(n) + G_f(v_{ra}(n) + v_{la}(n) - v_{rb}(n) - \\ &- v_{lb}(n)) \quad \forall n \in \{1, 2, \dots, N\} \\ h_{n+4N}(\mathbf{x}) &= Gv_{rb}(n) - G_f(v_{ra}(n) + v_{la}(n) - v_{rb}(n) - \\ &- v_{lb}(n)) \quad \forall n \in \{1, 2, \dots, N\} \\ h_{n+5N}(\mathbf{x}) &= Gv_{rc}(n) \quad \forall n \in \{1, 2, \dots, N\} \\ h_{n+6N}(\mathbf{x}) &= G(v_{ra}(n) - v_{ra}(n-2)) - \frac{2\Delta t\Lambda}{6}(v_{la}(n) + \\ &+ 4v_{la}(n-1) + v_{la}(n-2)) \quad \forall n \in \{1, 2, \dots, N\} \end{aligned}$$

$$\begin{aligned} h_{n+7N}(\mathbf{x}) &= G(v_{rb}(n) - v_{rb}(n-2)) - \frac{2\Delta t\Lambda}{6}(v_{lb}(n) + \\ &+ 4v_{lc}(n-1) + v_{lb}(n-2)) \quad \forall n \in \{1, 2, \dots, N\} \\ h_{n+8N}(\mathbf{x}) &= G(v_{rc}(n) - v_{rc}(n-2)) - \frac{2\Delta t\Lambda}{6}(v_{lc}(n) + \\ &+ 4v_{lc}(n-1) + v_{lc}(n-2)) \quad \forall n \in \{1, 2, \dots, N\} \end{aligned}$$

E. Delta Load without Fault

The sampled output of the system (illustrated in Fig. 2f):

$$\mathbf{y} = [\mathbf{v}_{ab} \ \mathbf{v}_{bc} \ \mathbf{v}_{ca} \ \mathbf{i}_a \ \mathbf{i}_b \ \mathbf{i}_c, \ \mathbf{z}_{ab} \ \mathbf{z}_{bc} \ \mathbf{z}_{ca}]^T$$

The state of the system:

$$x(t) = [G \ \Lambda \mathbf{v}_{rab} \ \mathbf{v}_{rbc} \ \mathbf{v}_{rca} \ \mathbf{v}_{lab} \ \mathbf{v}_{lbc} \ \mathbf{v}_{lca}]^T$$

The output function $\mathbf{h}(\mathbf{x})$ can be written as:

$$\begin{aligned} h_n(\mathbf{x}) &= v_{rab}(n) + v_{lab}(n) \quad \forall n \in \{1, 2, \dots, N\} \\ h_{n+N}(\mathbf{x}) &= v_{rbc}(n) + v_{lbc}(n) \quad \forall n \in \{1, 2, \dots, N\} \\ h_{n+2N}(\mathbf{x}) &= v_{rca}(n) + v_{lca}(n) \quad \forall n \in \{1, 2, \dots, N\} \\ h_{n+3N}(\mathbf{x}) &= G(v_{rab}(n) - v_{rca}(n)) \quad \forall n \in \{1, 2, \dots, N\} \\ h_{n+4N}(\mathbf{x}) &= G(v_{rbc}(n) - v_{rab}(n)) \quad \forall n \in \{1, 2, \dots, N\} \\ h_{n+5N}(\mathbf{x}) &= G(v_{rca}(n) - v_{rbc}(n)) \quad \forall n \in \{1, 2, \dots, N\} \\ h_{n+6N}(\mathbf{x}) &= G(v_{rab}(n) - v_{rab}(n-2)) - \frac{2\Delta t\Lambda}{6}(v_{lab}(n) + \\ &+ 4v_{lab}(n-1) + v_{lab}(n-2)) \quad \forall n \in \{1, 2, \dots, N\} \\ h_{n+7N}(\mathbf{x}) &= G(v_{rbc}(n) - v_{rbc}(n-2)) - \frac{2\Delta t\Lambda}{6}(v_{lbc}(n) + \\ &+ 4v_{lbc}(n-1) + v_{lbc}(n-2)) \quad \forall n \in \{1, 2, \dots, N\} \\ h_{n+8N}(\mathbf{x}) &= G(v_{rca}(n) - v_{rca}(n-2)) - \frac{2\Delta t\Lambda}{6}(v_{lca}(n) + \\ &+ 4v_{lca}(n-1) + v_{lca}(n-2)) \quad \forall n \in \{1, 2, \dots, N\} \end{aligned}$$

F. Delta Load with Line-Line Fault

The sampled output of the system (illustrated in Fig. 2d):

$$\mathbf{y} = [\mathbf{v}_{ab} \ \mathbf{v}_{bc} \ \mathbf{v}_{ca} \ \mathbf{i}_a \ \mathbf{i}_b \ \mathbf{i}_c, \ \mathbf{z}_{bc} \ \mathbf{z}_{ca}]^T$$

Note that there are no $z_{ab}(n)$ output variables as the reactive impedance on phase A is large compared to the parallel fault conductance G_f .

The state of the system:

$$x(t) = [G \ \Lambda \ G_f \ \mathbf{v}_{rab} \ \mathbf{v}_{rbc} \ \mathbf{v}_{rca} \ \mathbf{v}_{lbc} \ \mathbf{v}_{lca}]^T$$

where $G_f = R^{-1}$ is the conductance and the remaining states are the same as those in that of the delta no-fault state.

The output function $\mathbf{h}(\mathbf{x})$ can be written as:

$$\begin{aligned} h_n(\mathbf{x}) &= v_{rab}(n) \quad \forall n \in \{1, 2, \dots, N\} \\ h_{n+N}(\mathbf{x}) &= v_{rbc}(n) + v_{lbc}(n) \quad \forall n \in \{1, 2, \dots, N\} \\ h_{n+2N}(\mathbf{x}) &= v_{rca}(n) + v_{lca}(n) \quad \forall n \in \{1, 2, \dots, N\} \\ h_{n+3N}(\mathbf{x}) &= Gv_{ra}(n) \quad \forall n \in \{1, 2, \dots, N\} \\ h_{n+4N}(\mathbf{x}) &= Gv_{rb}(n) \quad \forall n \in \{1, 2, \dots, N\} \end{aligned}$$

$$h_{n+5N}(\mathbf{x}) = Gv_{rc}(n) \quad \forall n \in \{1, 2, \dots, N\}$$

$$h_{n+6N}(\mathbf{x}) = G(v_{rbc}(n) - v_{rbc}(n-2)) - \frac{2\Delta t\Lambda}{6}(v_{lbc}(n) + 4v_{lbc}(n-1) + v_{lbc}(n-2)) \quad \forall n \in \{1, 2, \dots, N\}$$

$$h_{n+7N}(\mathbf{x}) = G(v_{rca}(n) - v_{rca}(n-2)) - \frac{2\Delta t\Lambda}{6}(v_{lca}(n) + 4v_{lca}(n-1) + v_{lca}(n-2)) \quad \forall n \in \{1, 2, \dots, N\}$$

G. Delta Load with Line-Ground Fault

The sampled output of the system (illustrated in Fig. 2g):

$$\mathbf{y} = [\mathbf{v}_{ab} \quad \mathbf{v}_{bc} \quad \mathbf{v}_{ca} \quad \mathbf{v}_a \quad \mathbf{i}_a \quad \mathbf{i}_b \quad \mathbf{i}_c, \quad \mathbf{z}_{ab} \quad \mathbf{z}_{bc} \quad \mathbf{z}_{ca}]^T$$

The state of the system:

$$\mathbf{x}(t) = [G \quad \Lambda \quad G_f \quad \mathbf{v}_{rab} \quad \mathbf{v}_{rbc} \quad \mathbf{v}_{rca} \quad \dots]^T \\ [\dots \quad \mathbf{v}_{lab} \quad \mathbf{v}_{lbc} \quad \mathbf{v}_{lca} \quad \mathbf{v}_f]^T$$

where $G_f = R^{-1}$ is the fault conductance, \mathbf{v}_f is the voltage across the fault and the remaining states are the same as those in that of the delta no-fault state.

The output function $\mathbf{h}(\mathbf{x})$ can be written as:

$$h_n(\mathbf{x}) = v_{rab}(n) + v_{lab}(n) \quad \forall n \in \{1, 2, \dots, N\}$$

$$h_{n+N}(\mathbf{x}) = v_{rbc}(n) + v_{lbc}(n) \quad \forall n \in \{1, 2, \dots, N\}$$

$$h_{n+2N}(\mathbf{x}) = v_{rca}(n) + v_{lca}(n) \quad \forall n \in \{1, 2, \dots, N\}$$

$$h_{n+3N}(\mathbf{x}) = v_f(n) \quad \forall n \in \{1, 2, \dots, N\}$$

$$h_{n+4N}(\mathbf{x}) = G(v_{rab}(n) - v_{rca}(n)) + G_f v_f(n) \\ \forall n \in \{1, 2, \dots, N\}$$

$$h_{n+5N}(\mathbf{x}) = G(v_{rbc}(n) - v_{rab}(n)) \quad \forall n \in \{1, 2, \dots, N\}$$

$$h_{n+6N}(\mathbf{x}) = G(v_{rca}(n) - v_{rbc}(n)) \quad \forall n \in \{1, 2, \dots, N\}$$

$$h_{n+7N}(\mathbf{x}) = G(v_{rab}(n) - v_{rab}(n-2)) - \frac{2\Delta t\Lambda}{6}(v_{lab}(n) + 4v_{lab}(n-1) + v_{lab}(n-2)) \quad \forall n \in \{1, 2, \dots, N\}$$

$$h_{n+8N}(\mathbf{x}) = G(v_{rbc}(n) - v_{rbc}(n-2)) - \frac{2\Delta t\Lambda}{6}(v_{lbc}(n) + 4v_{lbc}(n-1) + v_{lbc}(n-2)) \quad \forall n \in \{1, 2, \dots, N\}$$

$$h_{n+9N}(\mathbf{x}) = G(v_{rca}(n) - v_{rca}(n-2)) - \frac{2\Delta t\Lambda}{6}(v_{lca}(n) + 4v_{lca}(n-1) + v_{lca}(n-2)) \quad \forall n \in \{1, 2, \dots, N\}$$

IV. EXPERIMENTS

Three different case-study systems are considered: 1) a single-phase load, 2) a grounded-wye constant-impedance load, and 3) a delta-connected constant impedance load. These load configurations are studied for both phasor-based state estimation and DSE. To verify the noise immunity of the methods, random noise with an amplitude of approximately 10% of the signal peak is added to the measurements in both cases. Experiments are performed in Julia v1.5 [14] and 64-bit MATLAB R2019b [15].

A. Phasor Implementation

For the single-phase phasor model, it is assumed that the source voltage is 240 [V] and the load impedance $R + jX$ is such that it draws a current of $10 - j5$ [A]. For the three-phase phasor models, both line-ground and line-line fault configurations are considered. These assume that the voltage source is 480 [V] rms line-line and the load impedance $R + jX$ is such that it draws $30 - j15$ [A] per phase. The fault resistance R_f is selected such that $R_f = R/10$.

Measured data is obtained by assuming a balanced input voltage and calculating the current by multiplying the input voltage phasor vector with the admittance matrix of the load-fault network. This is also the case for the single-phase dynamic load, however, in that case the measured phasor voltage is converted to instantaneous voltage to obtain the input for DSE.

B. Dynamic Implementation

The first case-study system is solved ad-hoc, assuming an ideal source with the parameters listed in Table I.

Variable	Symbol	Value	Units
Total load real power	P	10	kW
Total load reactive power	Q	5	kVAR
Line-line RMS source voltage	V_{ll}	480	V
Simulation time	T	10	ms
Sample rate	T_s	100	μs

TABLE I
PARAMETERS FOR SINGLE-PHASE DYNAMIC LOAD

The latter two case-study systems are modeled in the MATLAB/Simulink[®] SimScape multi-physics simulation environment, using the Specialized Power Systems library with the parameters listed in Table II and Table III.

Variable	Symbol	Value	Units
Total load real power	P	10	kW
Total load reactive power	Q	5	kVAR
Line-line RMS source voltage	V_{ll}	240	V
Source resistance	R_s	19.2	Ω
Source inductance	L_s	25.465	mH
Fault resistance	R_f	1	m Ω
Ground resistance	R_g	10	m Ω
Cable positive-sequence resistance	R_c	183.7	m Ω
Cable positive-sequence reactance	L_c	26.6	m Ω
Simulation time	T	200	ms
Fault start time	T_f	50	ms

TABLE II
COMMON PARAMETERS FOR THREE-PHASE DYNAMIC MODELS

Variable	Grounded-Wye	Delta
Load resistance R (Ω)	18.432	55.296
Load inductance L (mH)	24.457	73.3

TABLE III
VARYING PARAMETERS FOR THREE-PHASE DYNAMIC MODELS

In the systems, the load is connected to a 480 [V] rms line-line source through 1000 [ft] of 1/0 AWG quadruplex overhead service drop cable. Three different cases are considered: 1) no-fault, 2) line-ground fault, and 3) line-line fault.

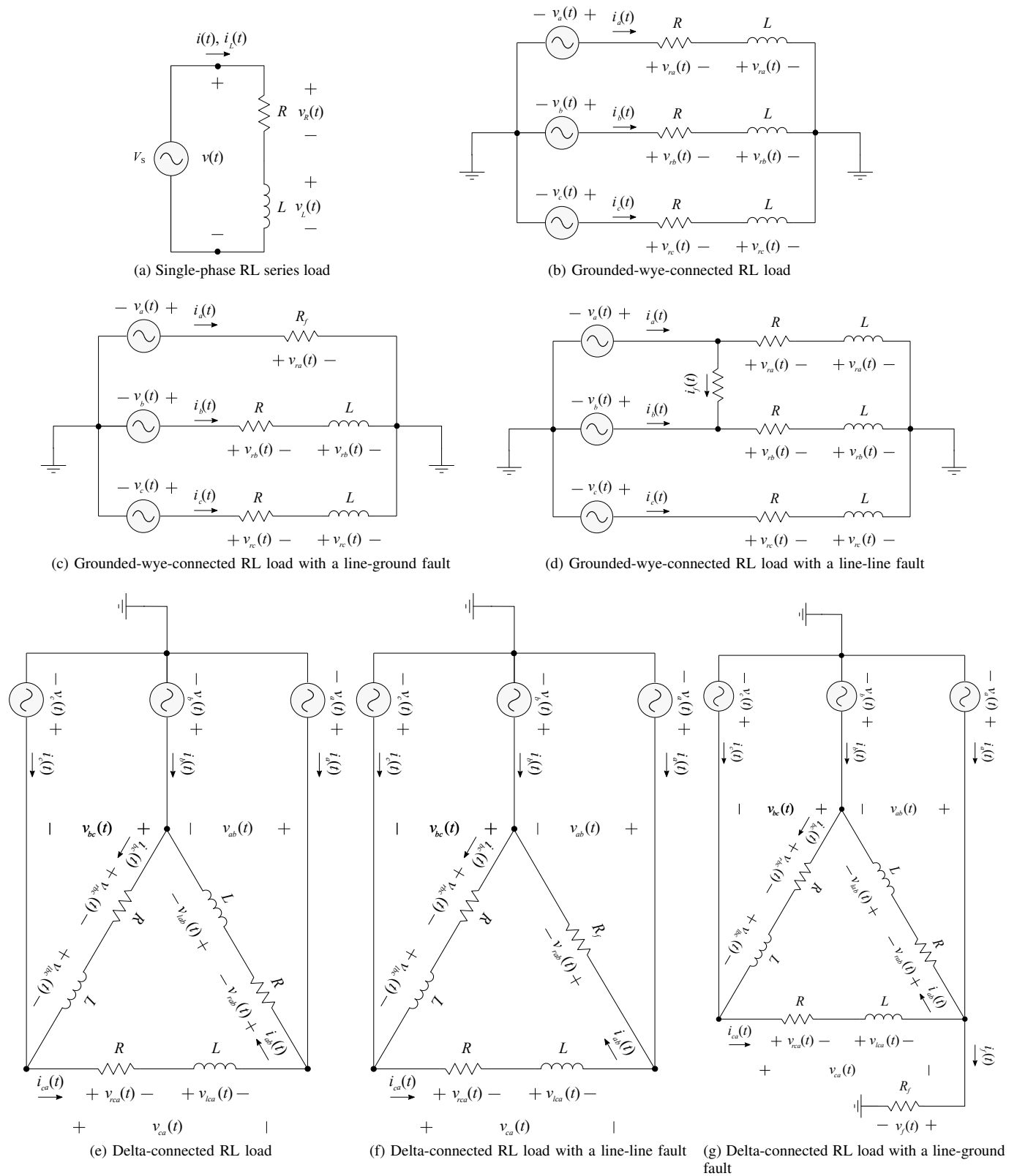


Fig. 2. Dynamic implementation of state estimation-based protection, applied to single-phase, grounded-wye and delta-connected load configurations.

C. Grounded-Wye Load

For the grounded-wye case, the system used is depicted in Fig. 3. The load consists of three balanced series RL branches wired in a grounded-wye configuration. This system has the parameters listed in Tables II and III. Note that the total fault resistance for the line-ground fault is $R_f + R_g = 110$ [m Ω], while the total fault resistance for the line-line fault is $2R_f = 200$ [m Ω].

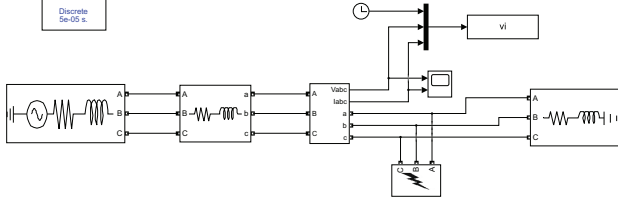


Fig. 3. MATLAB Simulink model for a grounded-wye load with faults.

D. Delta Load

For the delta-connected case, the system used is depicted in Fig. 4. The load consists of three balanced series RL branches wired in a delta configuration. This system has the parameters listed in Tables II and III. Note that the total fault resistance for the line-ground fault is $R_f + R_g = 110$ [m Ω], while the total fault resistance for the line-line fault is $2R_f = 200$ [m Ω].

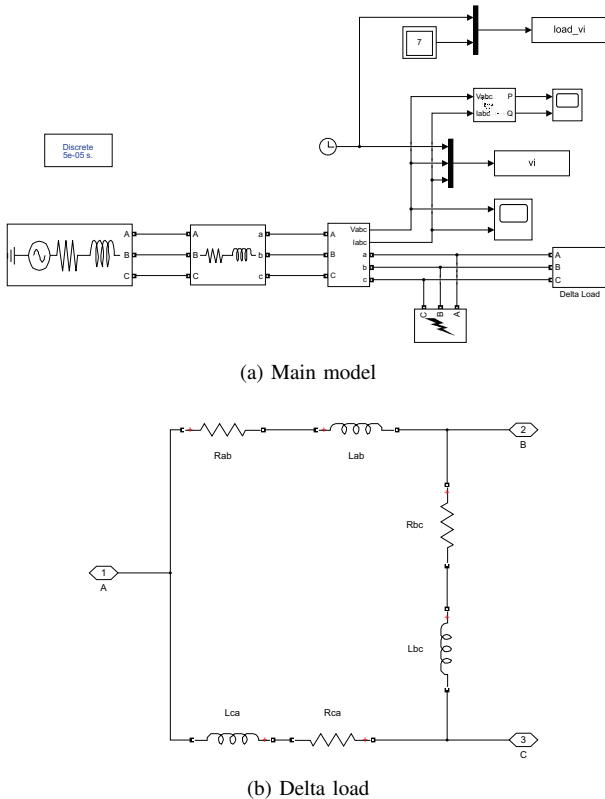


Fig. 4. MATLAB Simulink model for a delta load with faults.

V. RESULTS

Results for the phasor models are presented in Table IV, while results for the dynamic models are presented in Table V. The phasor models provide an excellent estimate of the system parameters. DSE has difficulty estimating the fault resistance for the dynamic model of grounded-wye network with a line-line fault; a potential solution is to reduce the model order by neglecting the load impedance on the faulted phases. Some moderate error is observed for the case of the delta-connected load with a line-ground fault; again, it may be possible to improve performance by neglecting load impedance on the faulted phases.

VI. CONCLUSIONS

The results of performed experiments prove that DSE is capable of correctly identifying model parameters of three different load configurations for both normal and faulted operations. These load configurations model a lumped equivalent of a radial electrical grid supplying multiple loads.

Several models showed sensitivity to initial conditions, particularly the delta-connected load, so it is important that consideration be given to providing the presented methods with good initial conditions. One issue is making sure that there is a sufficient number of measurements to estimate model states; for example, it is not possible to infer impedances for an unbalanced delta-connected load given a single time snapshot. To reduce the number of states, the models presented here assume that loads are balanced; this assumption can be an issue for systems with a high degree of load imbalance.

Existing work has demonstrated that DSE can operate with nonlinear elements [16]. One option for future work is to expand the here presented methods with other load models. These could include nonlinear voltage-dependent models where power is a polynomial function of voltage (ZIP loads) or where power is a polynomial function of both voltage and frequency (e.g. the WSCC load model [17]). Alternately, these could include dynamic load models (e.g. an induction motor model (MOTORW) or a composite load model (CMPLDW) [18]). Last, there is the possibility of protecting line sections that include loads with coordinated breakers at both ends; this could correspond to a distributed parameter line or a Pi/Tee lumped equivalent model [19].

Case	R	\hat{R}	X	\hat{X}	R_f	\hat{R}_f
Single-Phase RL Load	19.200	19.200	9.600	9.600	–	–
Grounded-Wye Line-Ground Fault	7.387	7.387	3.693	3.693	0.923	0.923
Grounded-Wye Line-Line Fault	7.387	5.184	3.693	4.787	0.923	0.935
Delta Line-Line Fault	22.160	22.160	11.080	11.080	2.770	2.770
Delta Line-Ground Fault	22.160	22.160	11.080	11.080	2.770	2.770

TABLE IV
RESULTS FOR PHASOR STATE ESTIMATION

Case	R (Ω)	\hat{R} (Ω)	L (mH)	\hat{L} (mH)	R_f (m Ω)	\hat{R}_f (m Ω)
Single-Phase RL Load	19.200	19.265	25.465	25.988	–	–
Grounded-Wye No Fault	18.432	18.404	24.446	24.485	–	–
Grounded-Wye Line-Ground Fault	18.432	18.432	24.446	24.446	11.000	10.997
Grounded-Wye Line-Line Fault	18.432	18.432	24.446	24.446	11.000	3.165
Delta No Fault	55.296	55.412	73.339	73.495	–	–
Delta Line-Line Fault	55.296	55.895	73.339	73.666	2.000	2.001
Delta Line-Ground Fault	55.296	55.479	73.339	73.495	11.000	11.405

TABLE V
RESULTS FOR DYNAMIC STATE ESTIMATION

REFERENCES

- [1] A. P. S. Meliopoulos, G. J. Cokkinides, P. Myrda, Y. Liu, R. Fan, L. Sun, R. Huang, and Z. Tan. Dynamic State Estimation-Based Protection: Status and Promise. *IEEE Transactions on Power Delivery*, 32(1):320–330, Feb. 2017.
- [2] Y. Liu, A. P. S. Meliopoulos, R. Fan, L. Sun, and Z. Tan. Dynamic State Estimation Based Protection on Series Compensated Transmission Lines. *IEEE Transactions on Power Delivery*, 32(5):2199–2209, 2017.
- [3] Y. Liu, A. P. S. Meliopoulos, L. Sun, and R. Fan. Dynamic State Estimation Based Protection of Mutually Coupled Transmission Lines. *CSEE Journal of Power and Energy Systems*, 2(4):6–14, Dec. 2016.
- [4] Y. Liu, A. P. S. Meliopoulos, R. Fan, and L. Sun. Dynamic State Estimation Based Protection of Microgrid Circuits. In *2015 IEEE Power Energy Society General Meeting*, pages 1–5, Jul. 2015.
- [5] O. Vasios, S. Kampezidou, and A. P. S. Meliopoulos. A Dynamic State Estimation Based Centralized Scheme for Microgrid Protection. In *Proceedings of the 2018 North American Power Symposium*, pages 1–6, Sep. 2018.
- [6] S. Choi and A. P. S. Meliopoulos. Effective Real-Time Operation and Protection Scheme of Microgrids Using Distributed Dynamic State Estimation. *IEEE Transactions on Power Delivery*, 32(1):504–514, Feb. 2017.
- [7] R. M. Tumilty, M. Brucoli, G. M. Burt, and T. C. Green. Approaches to Network Protection for Inverter Dominated Electrical Distribution Systems. In *Proceedings of the 3rd IET International Conference on Power Electronics, Machines and Drives, 2006*, pages 622–626, Apr. 2006.
- [8] M. Dewadasa, A. Ghosh, and G. Ledwich. Line Protection in Inverter Supplied Networks. In *Proceedings of the 2008 Australasian Universities Power Engineering Conference*, pages 1–6, Dec. 2008.
- [9] A. K. Barnes and A. Mate. Implementing Admittance Relaying for Microgrid Protection. In *Proceedings of the 2021 IEEE/IAS 57th Industrial and Commercial Power Systems Technical Conference*, pages 1–9, Apr. 2021.
- [10] J. M. Dewadasa, A. Ghosh, and G. Ledwich. Distance Protection Solution for a Converter Controlled Microgrid. In *Proceedings of the 15th National Power Systems Conference*, 2008.
- [11] D. P. Kothari and I. J. Nagrath. *Modern Power System Analysis*. Tata McGraw-Hill Education, 1989.
- [12] A. Monticelli. Electric Power System State Estimation. *Proceedings of the IEEE*, 88(2):262–282, Feb. 2000.
- [13] S. Chapra and R. Canale. *Numerical Methods for Engineers*. McGraw-Hill Education, 2009.
- [14] J. Bezanson, S. Karpinski, V. B. Shah, and A. Edelman. Julia: A Fast Dynamic Language for Technical Computing. *arXiv:1209.5145*, 2012.
- [15] MathWorks. MATLAB R2019b Documentation. *MATLAB* – <https://www.mathworks.com>, 2020.
- [16] H. F. Albinali. *State Estimation-Based Centralized Substation Protection Scheme*. PhD thesis, Georgia Institute of Technology, Aug. 2017.
- [17] L. Pereira, D. Kosterev, P. Mackin, D. Davies, J. Undrill, and Z. Wenchun. An Interim Dynamic Induction Motor Model for Stability Studies in the WSCC. *IEEE Transactions on Power Systems*, 17(4):1108–1115, Nov. 2002.
- [18] North American Electric Reliability Corporation. Technical Reference Document: Dynamic Load Modeling. Technical report, NERC, 2016.
- [19] D. T. Rizy and R. H. Staunton. Evaluation of Distribution Analysis Software for DER Applications. Technical report, Oak Ridge National Laboratory, 2002.